TRIGGER DESIGN FOR THE EAST OF ENGLAND SPARK CHAMBER

JONATHON WEI SING LEE

Clare College

JWSL2@cam.ac.uk

University of Cambridge, 2008 Undergraduate Research Opportunity

HEP Group, Cavendish Laboratory, J J Thompson Avenue, Cambridge, CB3 0HE

The recommended design for the East of England Spark Chamber is that of two photomultipliers with large photocathodes, Photonis XP3240s, each coupled directly to a 350mm x 500mm face of different 350mm x 500mm x 10mm slab of Eljen Technology EJ-200 PVT based scintillator. This design is recommended because it has the highest predicted collection efficiency by far, >11%, and is reasonably priced at approximately £1714.67.

CONTENTS

1 INTRODUCTION

1.1 Brief

The purpose of this UROP was to cost and evaluate trigger designs for the Cosmic Ray Spark Chamber for the East of England to be built at the High Energy Physics group at the Cavendish Laboratory. The brief specified by Dr C. G. Lester was:

"To research the interplay between the different scintillating materials (mainly doped plastics) currently commercially available, determine the wavelengths and amounts of light they produce (if any) when traversed by cosmic rays (by asking companies, reading data sheets, reading papers etc). To determine whether wavelength shifting fibres or blocks will be needed to be joined to or embedded in the primary scintillator to better match produced wavelengths to wavelengths which are more easily detected in the photon detectors, etc. To determine which wavelength shifting materials are appropriate (in terms of cost, input and output frequency matching etc). To determine the most appropriate photon detector to buy."

1.2 Cosmic Ray Spark Chamber for the East of England

Taken and edited with permission from:
http://www.hep.phy.cam.ac.uk/~lester/teaching/SparkChamber/SparkChamber.html (accessed 11/09/2008).

1.2.1 What is a Spark Chamber?

A spark chamber is a stack of conducting plates separated by a gas gap. When an energetic ionising particle passes through the device, a control circuit applies a high voltage between each pair of neighbouring plates. The voltage generates a spark between each of the plates. The spark prefers to form at the spot where the particle passed through, due to the ionisation trail left by the particle. The path of the traversing particle is thus revealed by the array or line of sparks, which may be seen or photographed through the side of the device. They hey-day of the spark chamber as a research tool for detecting high energy cosmic rays came to an end in the 1960s when it was replaced by better techniques (drift chambers, bubble chambers, silicon detectors etc). Nevertheless, spark chambers are still designed for museums and used in education as they are an exciting, visually direct and simple way of demonstrating cosmic rays to an audience.

1.2.2 Intended Impact

When a member of the public first sees a spark chamber in action, they are usually astonished. Although they may have heard of "Cosmic Rays" and "sub-atomic particles", they usually believe that these are ephemeral things that have nothing to do with reality.

A working spark chamber demolishes this notion instantly, demonstrating that each person is being "stabbed" in every minute of every day by a "cosmic rain" made of the same subatomic particles we observe in CERN. Adults and schoolchildren alike are astounded to learn that some of the particles generating the rays come from cataclysmic events in or outside the galaxy that are not yet understood by the science of today.

In two minutes, this piece of apparatus can:

(a) demonstrate the "reality" of particle physics,
(b) show the existence of sub-atomic particles,
(c) visualise real Cosmic Rays in real time,
(d) link particle physics "on earth" to astrophysics and astronomy "in space",

(e) excite people with the revelation that the source/existence of the highest energy cosmic rays is still a major topic of cutting-edge research, and remains largely unknown,
(f) encourage further discussion between demonstrators and the public on the work of CERN, astrophysicists and other STFC research areas.

1.2.3 Exploitation

Once built, the chamber will be used in three areas:

(a) The chamber will become a part of the CHaOS Road-Show (a multi-week summer event) and other CHaOS events throughout the year will take the chamber into schools, town halls and county shows around the country. To give an example of audience numbers: the 2007 "Road-Show" reached over 4000 people, and was accomplished over 20 days of demonstrating over a 4 week tour, and exhibited in Devon, Milton Keynes, Oxford, Nottinghamshire, Suffolk, Monmouthshire, Herefordshire and Lincolnshire. The annual "Crash Bang Squelch" event in Cambridge draws in a further crowd of 1000.
(b) The chamber will form the centrepiece of the Particle Physics contribution to "The Physics at Work outreach programme" which gains an annual attendance of 2100 schoolchildren, as well as any other smaller outreach days.
(c) The chamber will make its way to schools as a demo to support "schools talks" requested of suitably trained members of the Particle Physics staff.

1.2.4 Who will build/operate the Spark Chamber?

The Chamber will be built and operated by a joint venture between the High Energy Physics group of the Cavendish Laboratory of the University of Cambridge and the CHaOS Science Roadshow (Cambridge Hands-On Science Roadshow).

The Particle Physics group will supply the know-how, workshops, technicians, experience with HV safety, etc, to build the chamber, and is visited by 2100 school children annually in the "Physics at Work" events, thus guaranteeing at least this many visitors per year.

CHaOS has nearly ten years worth of experience of how to take scientific exhibits into schools, how to ensure safety, and most importantly knows how to construct something that can survive two weeks transport in the back of a van during a "CHaOS road show". Last year's "road show" visited eight counties and reached in excess of 4000 people.

Dr Lester (Cavendish Particle Physics) and Mr Ansell (CHaOS) will jointly "steer" the project over its lifetime. In addition, many other people will be involved in a variety of stages: providing advice, building it, demonstrating it, and providing training in demonstration.

Dr Lester will co-ordinate physics input to the design, liaise with experts in the Birmingham group (1), provide workshop space in which to build / store the detector, access to lab infrastructure and access to the experienced electrical/mechanical technicians and/or willing student labour. He also will demonstrate the chamber in Physics at Work days and on his own schools visits, and will train others in the use of the chamber. As an active member of the ATLAS experiment at the LHC, he will use the interest which spark chamber generates among members of the public to promote further discussion on particle physics, leading to further discussion of ATLAS and other LHC experiments.

Mr Ansell will provide input to the design, particularly regarding safety, transportability and accessibility. He will ensure that the chamber forms a key part of CHaOS events like the "road show" which will ensure the chamber gets to other parts of the country regularly. He will provide access to willing student demonstrators and science communicators, and provide training services to them. He may also put together smaller exhibits (e.g. Geiger counter + natural sources of radioactivity) that would complement the chamber and allow discussion of one to lead into the other - relating radioactivity, nuclear physics and particle physics.

Staff in the Cavendish will provide mechanical and electrical skills.

Students, members of staff and members of CHaOS will contribute to research, design, running, demonstrating and building the chamber.

1.2.5 Outreach / Publicity

Once the chamber is complete, Mr Ansell, in his role as a presenter of the "Naked Scientists Radio Show", will produce a short radio programme on the chamber (and an associated podcast). A typical "Naked Scientist" podcast is downloaded by 40,000 people, and the radio programme audience-size is in the region of 100,000.

A web-site to go with the chamber will be produced which would (a) inform other potential science communicators of a project that could be within their reach, and (b) communicate the aims of the project listed above to audience members who might never see the chamber in person.

Members of the local and/or national press are often invited to key outreach events at which the chamber will be present.

We do not expect to have to advertise the chamber *itself* within the target audience in order to gain audience numbers: the Physics at Work events and CHaOS "road-shows" are usually over-subscribed or fully booked, having been advertised by other organisations or by word of mouth via previous years.

1.2.6 Further Information

For more information on the following, please visit:

Cambridge University: http://www.cam.ac.uk

High Energy Physics, Department of Physics: http://www.hep.phy.cam.ac.uk

Cavendish Laboratory Outreach: http://www-outreach.phy.cam.ac.uk/physics_at_work/

Cambridge Hands-On Science: http://www.chaosscience.org.uk/pub/public_html/index.php

The Naked Scientist: http://www.thenakedscientists.com

The Birmingham Spark Chamber:
http://www.ep.ph.bham.ac.uk/general/outreach/SparkChamber/

The East of England Spark Chamber Project:
http://www.hep.phy.cam.ac.uk/~lester/teaching/SparkChamber/SparkChamber.html

2 COSMIC RAYS

The top of the atmosphere is bombarded by a great deal of cosmic radiation, the vast majority of which is extra-solar, origins still chiefly unknown. Cosmic rays have a very wide range of energies reaching beyond PeVs and consist largely of electrons, protons and nuclei synthesized inside stars. Such particles interact with the atmosphere creating all kinds of hadrons and leptons many of which subsequently decay or interact in the atmosphere to produce further hadrons and leptons.

2.1 Muons at Ground-Level

Of most interest to the Spark project are muons (arising from weak decays of charged hadrons) because they are easily detected by Spark chambers and interact weakly with matter compared to other charged particles so are the most abundant found at ground-level. The PDG (2) report that mean energy of muons at ground level is ≈ 4 GeV and that the "integral intensity of vertical muons above 1 GeV/c at sea level" ≈ 70 $m^{-2}s^{-1}sr^{-1}$, commenting that this corresponds to the "familiar" figure of $I \approx 1$ $cm^{-1}min^{-1}$ for horizontal detectors.

2.2 Muon Stopping Power

The ability of any trigger designed to 'see' muons is dependent upon the amount of energy muons will deposit in the bulk of the trigger. Therefore, the muon stopping power (for energies around 4 GeV) of materials for the trigger is of high importance. However, calculating the stopping power for even simple materials is highly non-trivial and is dependent on the energy regime of muons which itself is material dependent. The total stopping power requires the sum of the electronic stopping power and the energy dependent stopping power due to radiative processes (bremsstrahlung, e^+e^- pair creation and photonuclear interactions). In spite of this, Groom et al (3) have compiled a very comprehensive set of muon stopping power tables based upon both wide experimental and theoretical work, from which the stopping power of suitable trigger material has been taken.

3 SCINTILLATORS

There are many scintillating materials commercially available that emit electromagnetic radiation as traversing charged particles deposit energy in them. Scintillators can be divided into two types, organic and inorganic. In organic scintillators, fluorescence occurs due to transitions of electrons of the individual molecules and so is independent of the physical state of the scintillator whereas fluorescence occurs in inorganic scintillators due to the transitions of the electrons in the electronic states of the entire crystal lattice.

The ideal scintillator for the trigger will:

(a) have a high photon yield for cosmic ray muons, this requires:
    i. a high scintillation efficiency;
    ii. a high stopping power for muons in the low GeV energy range;
(b) be transparent to the radiation it emits;
(c) have a narrow emission spectrum that matches the peak sensitivity of the photon detector or the peak absorption of the wavelength shifting scintillator used (see 3.1.1);

(d) have a refractive index as close as possible to $n = 1.5$ for efficient coupling of scintillation light to the photon detector used (photon detector windows are typically made of borosilicate glass);
(e) be transportable;
(f) be inexpensive.

3.1 Plastic Scintillators

Plastic scintillators are made by dissolving an organic scintillator in a solvent which is then polymerized (4). Due to their ease of fabrication and shaping, plastic scintillators are commonly available commercially. Polyvinyltoluene (PVT) is typically used as the polymer base for plastic scintillators; its important properties are summarised in Table 1, for a comprehensive description of relevant PVT properties see Appendix A: PVT Muon Stopping Power.

Table 1 PVT Properties

Density /gcm^{-3}	1.032	Stopping Power for 4GeV Muons /MeVcm^{-1}	2.371
Refractive index	1.58		

Obtained from Groom et al (3) and Eljen Technology (5).

The stopping power is such that if the scintillating component of a PVT based scintillator emits at visible wavelengths and has an efficiency of only a few percent then it will yield several thousand photons per cm traversed by a muon of mean energy at ground level. Therefore, nearly all commercial plastic scintillators give suitably high photon yields for the trigger, so only those of low cost have been considered. Of suitable scintillators, the two cheapest are BC-408 (Saint-Gobain (6)) and EJ-200 (Eljen Technology (5)) their properties are given in Table 2 and their emission spectra in Figure 1.

Table 2 Plastic Scintillator Properties

	BC-408	EJ-200
Wavelength of Maximum Emission /nm	425	425
Bulk Light Attenuation Length /cm	380	380
Rise Time /ns	0.9	0.9
Decay Time /ns	2.1	2.1
Pulse Width (FWHM) /ns	~2.5	~2.5
Light Output /% of Anthracene	64	64
Scintillation Efficiency /photonsMeV^{-1}	not available	10000

Obtained from Saint-Gobain (6) and Eljen Technology (5).

The timings in Table 2 are not significant for the trigger (they would be if energy resolution was important) but are included to demonstrate how BC-408 and EJ-200 are indistinguishable by their properties that are available. Moreover, the emission spectra of the scintillators are very similar, though the accuracy of the spectra available are uncertain- the wavelength of maximum emission for BC-408 is given as 425nm yet appears on the

spectrum as 430nm. Due to the high degree of similarity between BC-408 and EJ-200 it is assumed that the scintillation efficiency for BC-408 is the same as that of EJ-200.

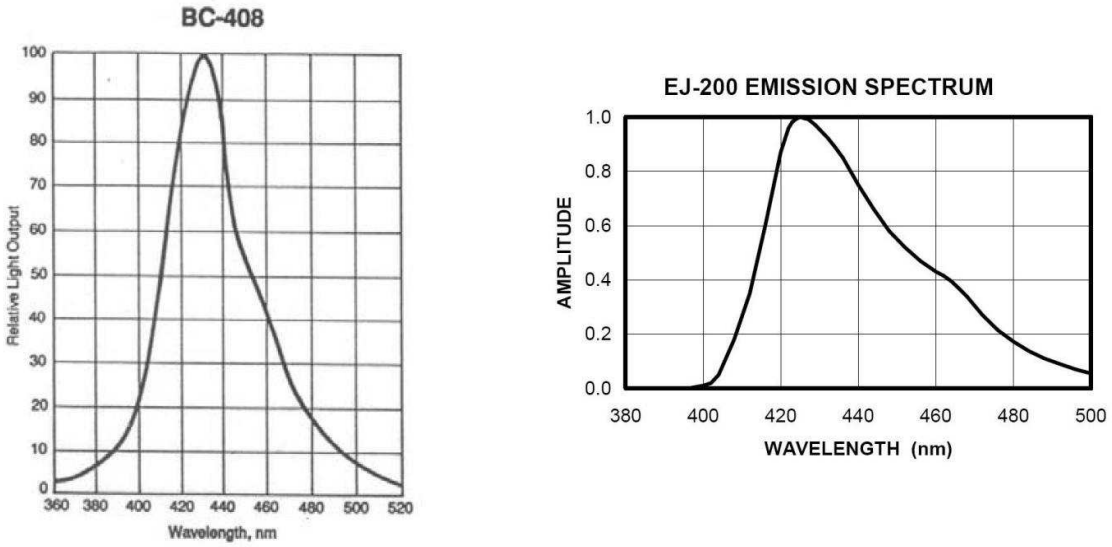

Figure 1
Emission spectra for BC-408 and EJ-200 from Saint-Gobain (6) and Eljen Technology (5) respectively.

These scintillators are well suited to the requirements of the trigger: they emit most intensely about 425nm which most photon detectors are sensitive to, the full width at half maximum (FWHM) of their emission peak is about 10% of the peak wavelength so is reasonably narrow, they have long attenuation lengths which allows for good collection of scintillation light, the refractive index of their PVT base is close to $n = 1.5$ so they couple well to photon detectors and the PVT base, though awkward to handle, is rugged enough to cope with vibration and small amounts of shock.

A further factor that affects the choice of scintillator is the finished form in which its available because the trigger requires slabs of scintillator with polished faces to maximise total internal reflection of scintillation light within the scintillator so that as much as possible can reach the photon detector. Both BC-408 and EJ-200 are available from their manufacturers diamond-tool-finished or saw-cut with excess scintillator along the faces that are to be polished. Polishing quite significantly affects the cost of the scintillator but polishing by hand is highly labour intensive and not as effective as diamond-tool-finishing. Many plastic manufacturing companies in the UK were contacted to see if they could diamond-tool-finish PVT, however none have handled PVT before but many were prepared to test a sample and may be able to polish the scintillator more cheaply than the manufacturers. Two plastic companies are preferred, Engineering and Design Plastics because of their local proximity (they are based in Cherry Hinton) and NE Plastics because they were recommended by two other plastic companies as experienced with plastics that are more exotic. Nevertheless, polishing by the manufacturers is recommended because of their natural experience in dealing with their own products.

In addition, it is possible to buy from Eljen Technology 'off-cuts' of EJ-200, which are batches of not sufficiently uniform thickness to pass their quality control checks but otherwise are like regular EJ-200, this is also available diamond-tool-finished or saw-cut. Prices for two slabs 350mm x 500mm x α mm of diamond-tool-finished and two slabs 360mm x 510mm x α mm

of saw-cut scintillator are given in Table 3 where $\alpha = 10\text{mm}$ for regular BC-408 and EJ-200 and $\alpha \approx 14\text{mm}$ for 'off-cut' EJ-200.

Table 3 Scintillator Prices

	BC-408	EJ-200	EJ-200 'off-cut'
Saw-cut	$ 660.00	$ 582.00	$ 396.00
Diamond-tool-finished	$ 1,080.00	$ 818.00	$ 632.00

Costs exclude VAT and P+P. Obtained from Eljen Technology and Saint-Gobain.

3.1.1 Wavelength Shifters

Secondary scintillators are often employed in trigger systems, these are wavelength-shifting scintillators that absorb the scintillation light from the primary scintillator and re-emit isotropically in a different part of the visible spectrum. Wavelength shifters, whilst reducing efficiency, in that their use adds an extra stage before photon detection, have advantages in terms of light collection and guiding. Wavelength shifters are utilised in two forms, either as a solid bar placed at a face of the primary scintillator or as fibres placed in grooves etched into the primary scintillator. Solid bars air-coupled to the primary scintillator pipe light by TIR more effectively to a photon detector than fibres, however fibres are more versatile easily fitting odd geometries and are significantly cheaper than solid bars since a comparatively smaller volume of fibre is used and no polishing is needed.

Blue (~420nm) to green (~490nm) wavelength shifters are the most suitable of those available because most photon detectors are sensitive to visible light in the blue-green range. Eljen Technology are the only company that could offer two wavelength shifting bars of dimensions 500mm x 10mm x10mm or 500mm x 15mm x 15mm for less than $1000. The properties of Eljen Technology's PVT based (see Table 1) EJ-280 wavelength shifter and cost are summarised in Table 4. Only Saint-Gobain could offer any wavelength shifting fibres and they require a minimum spend of $400, the properties of their BCF-91A fibre is given in Table 4.

Table 4 Properties and Cost of EJ-280 and BCF-91A

EJ-280		BCF-91A	
Wavelength of Maximum Absorption /nm	425	Wavelength of Maximum Absorption /nm	420
Wavelength of Maximum Emission /nm	490	Wavelength of Maximum Emission /nm	494
Maximum Quantum Efficiency /%	86	Maximum Quantum Efficiency /%	Not available
Bulk Light Attenuation Length /cm	350	Light Attenuation Length /cm	350
Cost of 2 saw-cut bars	$ 178.00	Available diameters /mm	0.25 to 5
Cost of 2 diamond-tool-finished bars	$ 424.00	Minimum bending radius	x25 fibre diameter
		Cost per m for <200m of 1mm fibre	$ 4.15

Costs exclude VAT and P+P. Obtained from Eljen Technology (5) and Saint-Gobain (6).

The absorption and emission spectra of EJ-280 and BCF-91A are presented in Figure 2. The overlap between the absorption and emission spectra for both EJ-280 and BCF-91A are sufficiently small that it seems self-absorption will have a negligible effect on overall efficiency in any trigger design in which either are used.

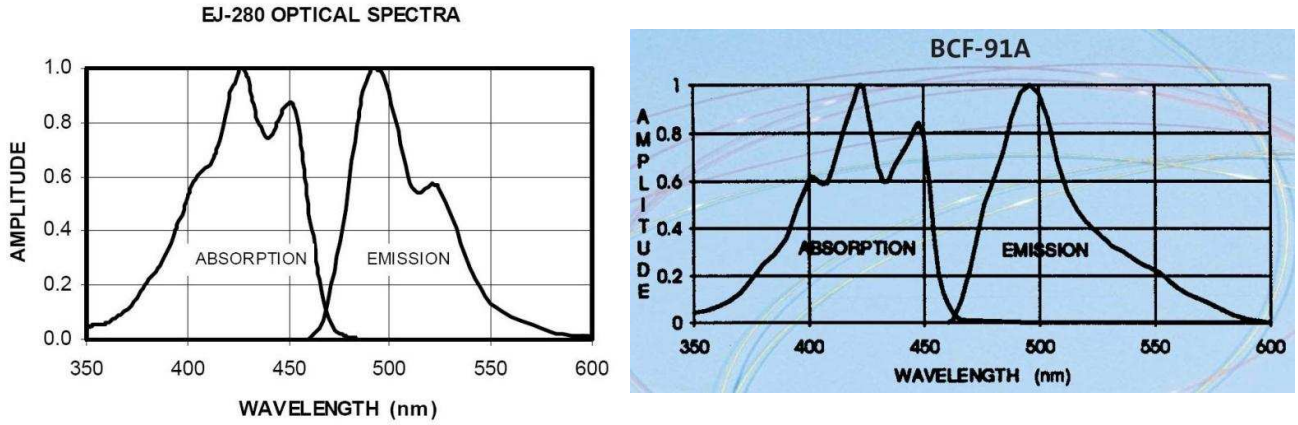

Figure 2
EJ-280 and BCF-91A Absorption and Emission Spectra from Eljen Technology (5) and Saint-Gobain (6) respectively.

3.2 Crystal and Liquid Scintillators

Both inorganic crystal and organic liquid scintillators were recognised as inappropriate for the trigger. Inorganic crystals generally have the best scintillation efficiencies and stopping powers (due to their higher densities). However, they are suitable only for small detectors because their attenuation lengths are typically quite short and crystals of dimensions suitable for the trigger either cannot be grown or cost of the order of tens of thousands of pounds. Moreover, inorganic crystals typically have refractive indices of $n > 1.8$ which limits the coupling efficiency to photon detectors and are not very rugged and therefore not very transportable. Conversely, organic liquid scintillators are very inexpensive and typically have refractive indices close to $n = 1.5$ so scintillation light couples very well to photon detectors. Organic liquid scintillators are inappropriate for the trigger, though, because liquid scintillators must be kept in vacuum-sealed containers (dissolved gas in the liquid worsens the scintillation efficiency acutely) and such containers are typically bulky and massive limiting transportability.

4 PHOTON DETECTORS

All photon detectors operate on the basis of converting incoming photons into an electrical signal either by liberating electrons from a material with a suitably chosen ionisation energy or by promoting electrons in a material with a suitably chosen band gap and accelerating and multiplying these electrons. For a long time photomultiplier tubes have dominated photon detection and they continue to do so, however semiconductor based solid state devices are competing increasingly well with photomultipliers are on several fronts.

The ideal photon detector for the trigger will:

(a) have a high quantum efficiency/radiant sensitivity for the wavelength of maximum emission of scintillator (or wavelength shifter) used;

(b) have a high gain;
(c) have low noise levels;
(d) operate from a 15V supply;
(e) be compact and reasonably rugged;
(f) have a photocathode size appropriate for the trigger design;
(g) be inexpensive;

4.1 Photomultipliers

Photomultipliers (PMs) operate by incident photons liberating electrons from a photosensitive cathode that is connected to an electron multiplier, which turns the small number of liberated electrons into a signal of around 10^7 to 10^{10} electrons (4) read out at the anode. There are numerous PMs commercially available, many of which are sensitive to the blue-green part of the visible spectrum that the scintillators considered emit in, with a very wide range of photocathode sizes and gains of around 10^6. Typical PMs are bulky and require a separate high voltage power supply (HV PS), in addition to cost these are very important factors to the trigger.

Photomultiplier modules (PMMs) are well suited to the trigger because they integrate a PM with a HV PS in a compact way and are normally cheaper than buying a PM and HV PS separately. However, PMMs are more limited in available photocathode size and price does increase strongly with increasing photocathode size. Hamamatsu Corporation (7) produces the widest range of and cheapest PMMs, all of the recommended PMMs are assembled by them. Table 5 contains the properties of the H6780, H7826 and H8443 PMMs and their cathode radiant sensitivities against wavelength are shown in Figure 3.

Assemblies of a PM and custom HV PS are the best compromise between size of photocathode and external size of the photon detector where PMMs would be too expensive (i.e. very large photocathode sizes). Only one assembly researched is suitable for the trigger and of a comparable price to the Hamamatsu PMMs, it consists of a XP3240 from Photonis and a PS1809 from Sens-Tech. The combined properties of the XP3240 + PS1809 assembly are also given in Table 5 and the cathode radiant sensitivity against wavelength of the XP3240 is shown in Figure 3.

Table 5 Properties of Selected Photomultipliers

PMM or Assembly	H6780	H7826	H8443	XP3240 + PS1809
Photocathode Active Diameter /mm	8	15	22	46
Peak Sensitivity Wavelength /nm	420	420	420	420
Cathode Radiant Sensitivity at 420nm /mA/W 490nm /mA/W	62 52	85 70	88 68	75 58
Typical Anode Radiant Sensitivity at 420nm /A/W 490nm /A/W	4.3×10^4 3.6×10^4	4.7×10^4 3.9×10^4	1.7×10^5 1.3×10^5	5.3×10^4 4.1×10^4
Anode Dark Current /nA Typ (Max)	0.2 (2)	3 (20)	2 (15)	0.5 (2)
Anode pulse FWHM /ns	1.57	2.5	2.6	12
Mass /g	80	70	210	240
Maximum External Dimensions /mm	22 x 22 x 50	26 x 50 x 56	ø34 x 121	ø59.5 x 189
Cost	£350	£445.50*	£495	€218.80* + £280 = £458.12

*- includes 10% discount. Underlined dimension denotes the dimension perpendicular to the photocathode. All costs exclude VAT and P+P. Obtained from Hamamatsu, Photonis and Sens-Tech.

The choice of PM depends most significantly on choice of design and the tolerability of disadvantages such as mass and size to the trigger requirements. The advantages and disadvantages of the PMs considered in Table 5 are:

- H6780 is the cheapest, the smallest, has the lowest rate of accidentals and a small mass. However, it has the worst anode radiant sensitivity.
- H7826 is the lightest and is small with a larger photocathode than H6780. However, it has the highest rate of accidentals, it has worse anode radiant sensitivity than H8443 in green (490nm) and XP3240 in blue (420nm)- the PMs it would compete against in two designs (see 5.1.1 and 5.1.2).
- H8443 has the best anode sensitivity by more than a factor of 3 compared to the other PMs. However, it is the most expensive, is more than 2.5 times the mass of H6780 and H7826 and is more than twice as long as they are in the dimension that would project out from the scintillator edge.
- XP3240 has the largest photocathode, more than 4 times the area of and is cheaper than H8443 the next largest. However, it is heavier and is more than 50% longer in the protruding direction than H8443.

To compare the PMs' accidental rates- the rate of coincidence due to random overlap of false signals- one considers the anode dark current- the time average of electrons arriving at the anode from spontaneous electron emission by the photocathode due to thermionic noise. This dark current is what leads to false signals at the output of the photomultiplier, which is why two sets of scintillator and PM must be employed so that only coincident signals are considered. Approximately, the accidentals rate is proportional to the product of the dark current and pulse width so the accidentals ratio for H6780 to H7826 to H8443 to XP3240 is 1 : 24 : 17 : 19.

Figure 3 shows the general similarity in shape of response of the PMs across the wavelengths shown. From 400nm to 525nm, the range of wavelengths that covers the FWHM of the emission spectra of all of the primary and secondary scintillators considered, none of the PMs fall in sensitivity below half that of their peak sensitivity. Therefore, the sensitivities in Table 5 are sufficiently representative of the PMs that factors due to the shape of sensitivity against wavelength are negligible.

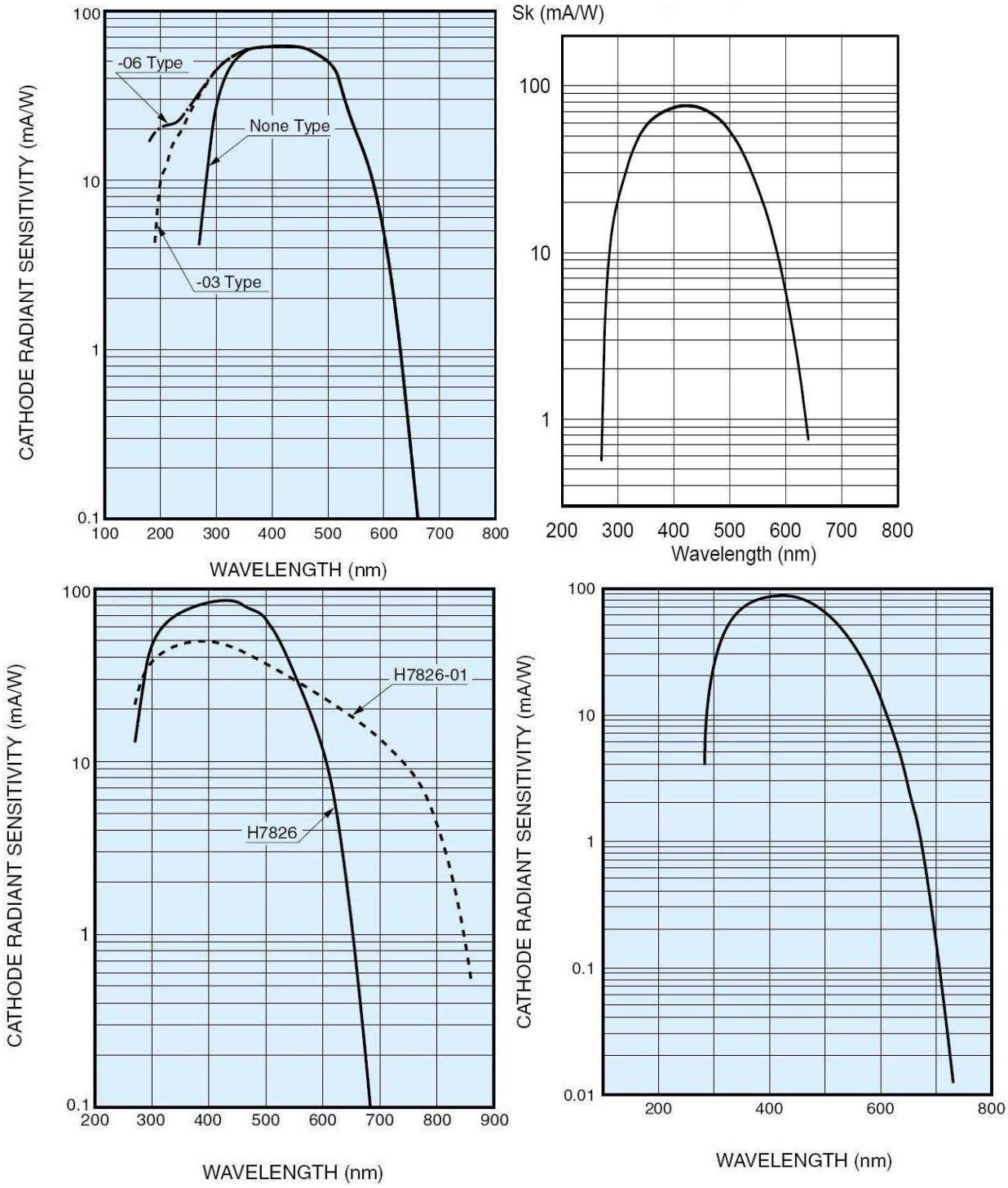

Figure 3
Cathode Radiant Sensitivity against Wavelength for: (Clockwise from top-left) H6780, H7826, H8443, XP3240. Obtained from Hamamatsu (7) and Photonis. The “-03 Type”, “-06 Type” (top left) and the “H7826-01” (bottom left) are not relevant.

4.2 Avalanche Photodiodes

Avalanche photodiodes overcome many of the disadvantages of typical photomultipliers (4): they are unaffected by magnetic fields, have high quantum efficiencies (typically 80%), are

less bulky, are more rugged and do not require HV power supplies. Except for the first quality, all of these advantages are relevant to the trigger. However, there are three disadvantages of avalanche photodiodes that together disqualify them from recommendation for the trigger: the amplification provided by an avalanche photodiode is typically a few orders of magnitude less than by a photomultiplier; they are not readily available with active diameters much greater than 5mm; and they are not as cheap the photomultipliers considered above.

5 TRIGGER DESIGNS

5.1.1 Bare Scintillator

This is the simplest design, two 350mm x 500mm x 10mm (or ~14mm) slabs of EJ-200 each with a PM optically coupled directly to part of one of the 350mm x 10mm (or ~14mm) faces of each see Figure 4.

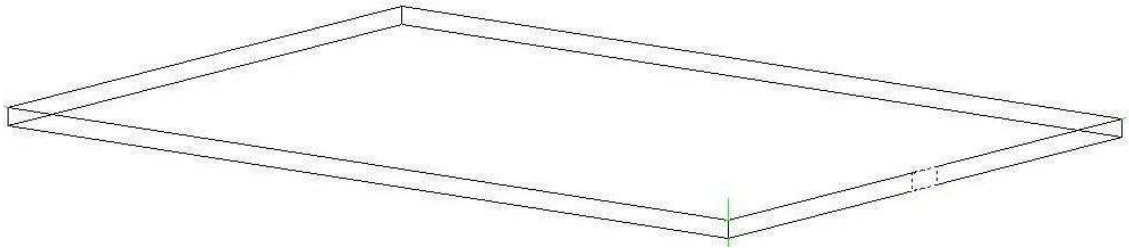

Figure 4
Bare scintillator model used in ray tracing, the dotted area denotes, in this case 10mm x 22mm of photocathode.

A variation on this design to accommodate longer PMs (i.e. the XP3240) is to couple the PMs to the bottom face of the top scintillator and the top face of the bottom scintillator (see Figure 5).

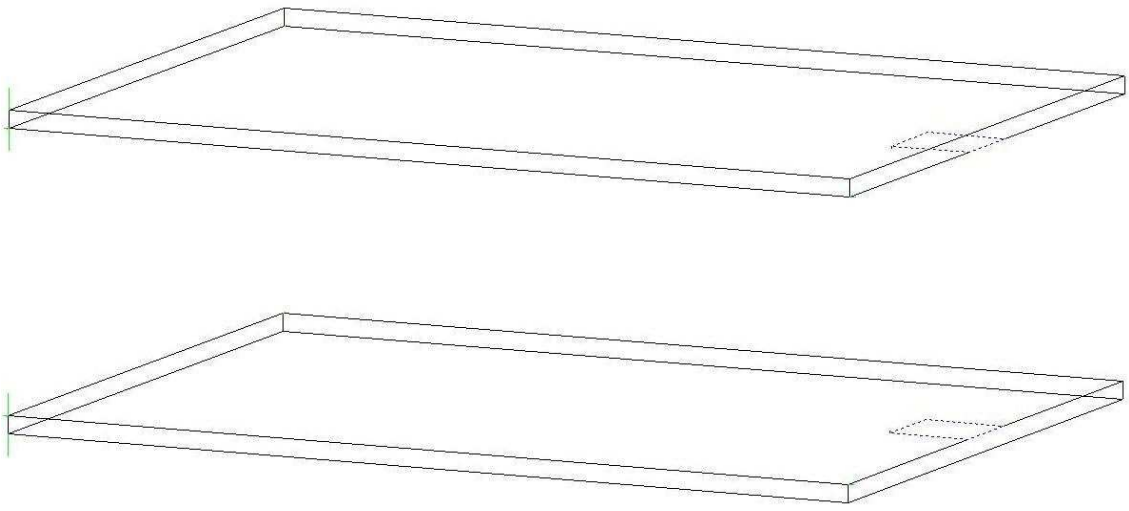

Figure 5
Bare scintillator variation for long PMs, the dotted area denotes, in this case 46mm x 46mm of photocathode.

5.1.2 WLS bar

A wavelength shifting scintillator is most easily utilised in bar form. This second design has two 350mm x 10mm x 10mm (or 15mm x 15mm) bars of EJ-280 each attached to a 350mm x 500mm x 10mm (or ~14mm) slab of EJ-200 with a small air gap so that as much green light emitted by EJ-280 as possible will be piped by TIR to a PM see Figure 6. For the PM to be large enough for the exit face of the WLS bar, it must have a diameter greater than 14mm (or 21mm).

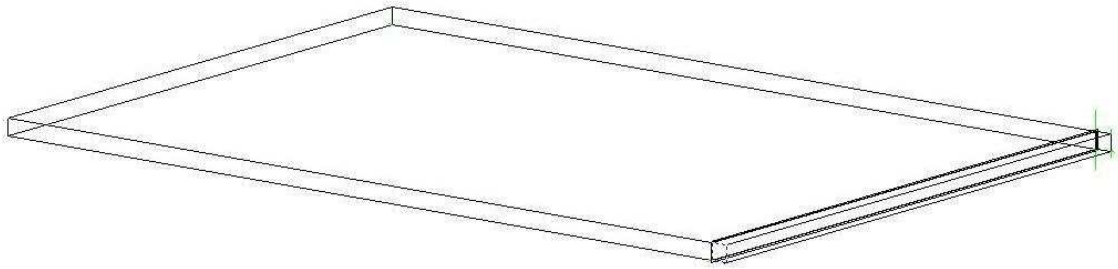

Figure 6
WLS bar model used in ray tracing, the dotted area denotes the end of the bar to be optically coupled to the photocathode.

5.1.3 WLS fibre

This third design is more complicated as it requires the etching of circular grooves (by the manufacturers) in two 350mm x 500mm x 10mm (or ~14mm) slabs of EJ-200 into each of which turns of 1mm diameter, mulitclad, BCF-91A are bonded with optical cement with the ends optically coupled to two H6780s (the smallest PM) see Figure 7.

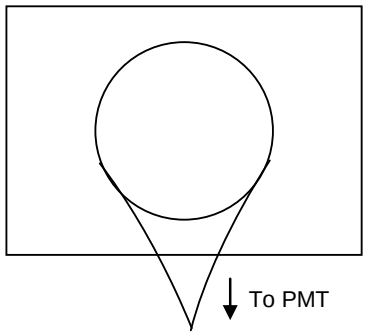

Figure 7
A sketch of the WLS Fibre design from above.

5.1.4 Scintillating Fibre

A fourth design is to have no slab of scintillator at all but to use an amount of scintillating fibres of comparable volume to a slab. This has a few advantages, over all of the designs discussed so far, that mean significantly more photons reach the photomultiplier. Firstly, a greater utilisation of TIR with light piped by many fibres rather than reflected around within a slab. Secondly, with the large area photocathode, XP3240, all of the fibres making up the volume could be coupled to it directly (the fibres effectively form their own adiabatic light guide). Thirdly, no secondary scintillator is required nor a light guide so it has the least number of stages from scintillation to arriving at the photocathode. However, this design is

not feasible on cost grounds: the cheapest that the required amount of scintillating fibre could be obtained for is $1950 (exc VAT and P+P).

5.2 Collection Efficiency

To establish which design is best, the fraction of the total primary scintillation light that reaches the photocathode must be considered. A ray tracing program (see Appendix B: RaySim6.0) has been used to determine the mean amount of scintillation light from a 350mm x 500mm x 10mm scintillator that will reach PMs of various photocathode widths placed in the middle of a 350mm edge and also used to determine the mean amount of scintillation light that will reach a 350mm x 10mm x 10mm WLS bar air coupled to a 350mm edge. Due to the limitations of the ray tracing program such simulations could not be run for the WLS fibre design, however using geometrical arguments one can place limits on the WLS fibre design that allow comparison with the others.

The results from the ray-tracing program are given in Table 6. The PM results are corrected to account for the circular photocathodes by a simple geometric factor that is the actual area of the photocathode in contact with the scintillator divided by the simulated area. Simulations were also run for the 'worst case' of a few set-ups, this involved placing a single point source in the position where one intuitively expects the least light to reach the PM (see note on Table 6).

Table 6 Ray Tracing Results with Correction

Simulation		8mm x 8mm	10mm x 22mm	10mm x 46mm	46mm x 46mm	WLS Bar
Total Fraction of Light Absorbed	Mean	0.01486	0.04847	-	-	0.08754
	Worst Case*	0.008149	0.03761	0.07238	0.1455	-
Geometric Correction Factor		0.7854	0.9644	0.9912	0.7854	None
Corrected Fraction	Mean	0.0117	0.0467	-	-	0.08754
	Worst Case*	0.00640	0.0363	0.0717	0.114	-

*A point source 25mm from one of the 500mm edges and 25mm from the same 350mm edge as the PM for 10mm x 46mm and 25mm from the opposite 350mm edge as the PM for 46mm x 46mm (the source was not place right in the corner because the slab was divided into 70 50mm x 50mm 'pixels'). Unfortunately, time constraints meant ray tracing could not be performed for a 15mm diameter photocathode or the mean for a 46mm diameter photocathode or 46mm variation. NB these results include self-absorption by the scintillator.

To estimate the collection efficiency of the WLS bar, the corrected fraction of light absorbed must be multiplied by a factor due to the emission spectrum of EJ-200 (see Figure 1) and the absorption spectrum (see Figure 2) and quantum efficiency of EJ-280. This factor was calculated by normalising the area under the emission spectrum of EJ-200 to unity, multiplying this by the absorption spectrum of EJ-280 (which is normalised such that the peak has unity amplitude) and multiplying this by 0.86 (=Peak QE of EJ-280). Not all of the light emitted by the secondary scintillator will reach the PM; using solid angle arguments taking TIR into account there is a further factor of 0.2046. This gives a mean collection efficiency for the WLS bar design of

$$\overline{CE}_{Bar} = 0.08754 \times 0.6807 \times 0.86 \times 0.2046 = 1.0\% \quad (2\text{sf}).$$

However, this result and the values given above for the bare scintillator are not the actual collection efficiencies, reflection due to the difference in the refractive indices of the scintillator or WLS bar and the PM window must be considered. To estimate the worst possible value of this factor the critical angle for the scintillator to air interface is taken from π/2 and put into the Fresnel reflection formulae with the refractive indices of the scintillator (1.58) and the borosilicate glass of the PM windows (1.50), the result of which is subtracted from unity. This is reasonable because π/2 minus the scintillator to air critical angle is the maximum angle of incidence for scintillation photons on a scintillator/WLS bar to PM window interface. This factor turns out to be 0.9975, which has a negligible effect on the overall collection efficiencies, which are

$$\overline{CE}_{Bar} = 1.0\% \quad \overline{CE}_{\text{ø8mm}} = 1.2\% \quad \overline{CE}_{\text{ø22mm}} = 4.7\%$$

$$CE_{\text{ø46mm}} \geq 7.2\% \quad CE_{\text{Var ø46mm}} \geq 11\% \quad (\text{all 2sf}).$$

These results are all lower limits to some extent, as this does not take into account the wrapping external surfaces of the trigger in reflective foil, which will increase the amount of light collected by the PM for all designs. Nevertheless, the simulations cannot take into account slight irregularities in the finish of the scintillator and the presence of impurities, though one hopes these things will have no effect to the level of significance considered.

Performing similar calculations for the WLS fibre

$$\overline{CE}_{Fibre} = F \times 0.5812 \times QE \times 0.056 \times 2 \times 0.9989 = F \times QE \times 6.5\% \quad (2\text{sf}).$$

Where F is the fraction of light absorbed by the WLS fibre from the scintillator, 0.5812 is the factor from the multiplication of the emission spectrum of EJ-200 and the absorption spectrum of BCF-91A, QE is the peak quantum efficiency of BCF-91A, 0.056 is the minimum trapping efficiency of multi-clad BCF-91A, 2 to account for both ends of the fibre being coupled to the PM and 0.9989 to account for the difference in the fibre core (1.60) and PM window (1.50) refractive indices. Assuming QE = 0.86 (i.e. the same as EJ-280) then

$$\overline{CE}_{Fibre} = 5.6F\% \quad (2\text{sf}).$$

Solid angle and TIR arguments limit F to be less than 0.7742; this implies it is impossible for the WLS fibre design to match the bare scintillator design with a photocathode of 22mm or 46mm diameter and to match the WLS bar F must be 23% of this maximum value. Supposing F is approximately directly proportional to the number of turns of WLS fibre, where 10 turns would have an F of 0.7742 the maximum value because 10 turns covers the depth of the scintillating slab. Though, this many turns is not preferable for that reason, that it would require the scintillator to be cut into two separate pieces which would significantly decrease the strength of the slab plus fibre increasing the risk of damage during transport. To achieve comparable collection efficiencies to the WLS bar and the bare scintillator with the 8mm diameter photocathode, 3 turns are required.

These results are very surprising as it is 'conventional wisdom' that a wavelength shifter is to be preferred over direct scintillator PM coupling. However, this may be due to reasons not important to the trigger such as: space and geometry issues, where a photon detector cannot be joined to the scintillator; magnetic field issues, where the photon detectors need to be far away and shielded from a magnetic field near to the scintillator; or energy resolution

issues, where the scintillation pulse needs to have a smaller width than that of light that is reflected many times and has travelled some distance before reaching the PM. For example, the Tile Calorimeter in the ATLAS detector (8) has many of such things to consider so has WLS fibres on the edge of scintillating tiles reading out to PM radially further out from the beam pipe than the tiles.

Finally, for photon yield one has to consider the use of 'off-cut' scintillator, with mean thickness 14mm, instead of regular scintillator. Energy deposited by muons over short ranges (i.e. over the scintillator thickness) is linear so one expects a 40% greater photon yield from 14mm thick 'off-cut' compared to 10mm thick regular scintillator. From 10mm scintillator one expects 24000 scintillation photons (2sf) and from 14mm 33000 (2sf). However, due to the non-uniform thickness of the off-cut scintillator, there will be less TIR from the top and bottom faces than for regular scintillator, though the significance of this effect is impossible to estimate because the level of irregularity is unknown.

Overall for each design using regular scintillator the numbers of photons reaching the PM are

$$N_{Bar} = 240 \quad N_{\text{ø8mm}} = 290 \quad N_{\text{ø22mm}} = 1100$$

$$N_{\text{ø46mm}} \geq 1900 \quad N_{\text{Var ø46mm}} \geq 2600 \quad N_{Fibre} \approx 100 \times \#\,\text{of turns} \quad (\text{all 2sf}).$$

Using N_{bar} the lowest estimate of PM output can be calculated. Choosing a serious underestimate of the factor to account for the difference in all of the light reaching the PM not all being of the wavelength of peak sensitivity of say 0.4 and multiplying this by N_{bar}, the energy per peak photon, the reciprocal of the photon arrival time spread and the peak radiant sensitivity of H7826 gives the output current. This current will then be terminated by 50Ω giving an output signal of

$$V = 0.4 \times 240 \times \frac{\text{hc}}{425 \times 10^{-9}\text{nm}} \times (10^{-9}\text{s})^{-1} \times 4.7 \times 10^{4}\text{A/W} \times 50\Omega = 10\text{mV} \quad (1\text{sf}).$$

The magnitude of this signal is adequate to be resolved by the circuitry planned to be used for the trigger, so this does not eliminate any design choice.

5.3 Cost Summary

Cost will strongly influence which design is chosen and which of the suitable components for each design are selected. See Table 7 for the estimated full costs of each possible combination of components featured in this report, for each of the designs in 5.1.1 to 5.1.3 the recommended components with their total cost are each given in Table 8.

Table 7 Trigger Cost Summary

		Scintillator						
		EJ-200				+EJ-280 WLS bar		+SG BCF-91A WLS fibre
		Off-cut		Regular		Regular		1mm diameter, multi-clad
		Saw cut	Diamond-polished	Saw cut	Diamond-polished	Saw cut	Diamond-polished	
PM	H6780 (8)	£1,119.57	£1,275.60	£1,242.55	£1,398.58	-	-	+£279.46
	H7826 (15)	£1,343.99	£1,500.03	£1,466.97	£1,623.00	+£117.69	+£280.33	-
	H8443 (22)	£1,460.32	£1,616.35	£1,583.30	£1,739.33	+£117.69	+£280.33	-
	Ph XP3240 +ST P1809 (46)	£1,435.66	£1,591.70	£1,558.64	£1,714.67	+£117.69	+£280.33	-

Brackets denote photocathode active diameter; '-' denotes a combination strongly not recommended. H- Hamamatsu, ST- Sens-Tech, Ph- Photonis, EJ- Eljen Technology, SG- Saint-Gobain. Prices include VAT and estimated P+P, where necessary the exchange rates at 13:30 GMT 3/09/2008 of $1 = £0.56269 and €1 = £0.81408 were used.

Table 8 Recommended Components and Estimated Cost for each Trigger Design

Design	Components	Total Cost
Bare Scintillator	Regular, diamond-polished EJ-200 + XP3240 + P1809	£1,714.67
WLS bar	Regular, diamond-polished EJ-200 + diamond-polished EJ-280 + H8443	£1,903.33
WLS Fibre	Regular, diamond-polished EJ-200 + BCF-91A + H6780	£1,678.04

6 CONCLUSION

There are three main designs for the trigger for the East of England Spark Chamber- (a) scintillator and PM alone, (b) scintillator, WLS bar and PM and (c) scintillator, WLS fibre and PM. Each can be constructed with a variety of viable components; of the sensible configurations, none is more expensive than £1903.33. The best design in terms of light collection efficiency is that of scintillator plus the PM with the largest photocathode, XP3240 in the 'variation' design and at £1591.70 or £1714.67 for off-cut or regular EJ-200, the design is cheap to medium in price. The WLS fibre design is cheaper but the collection efficiency cannot approach that of the bare scintillator design with large photocathode. The WLS bar design is too expensive in comparison with the others; especially given it has the worst light collection efficiency. For all designs, manufacturer diamond-tool-polishing of the scintillator is recommended because of their experience with their own products, unless a plastics company can prove they can handle PVT and polish it without causing crazing and for significantly cheaper than the manufacturer.

The recommended design for the trigger for the East of England Spark Chamber is the 'bare scintillator variation' design with regular, diamond-polished EJ-200 from Eljen Technology, XP3240s from Photonis and P1809s from Sens-Tech. This design is best because it has the greatest predicted collection efficiency of at least 11% and simple because there is no secondary scintillator. Moreover, with regular, diamond-polished scintillator from the manufacturer one can be confident that the actual collection efficiency will be close to the predicted value, compared to off-cut or not manufacturer polished, where one expects less TIR. However, the design is neither the cheapest, nor the least bulky but a high collection efficiency that one can have a little confidence in attaining is worth it for the trigger.

APPENDIX A: PVT MUON STOPPING POWER

This table from Groom et al. (3) summarises theoretical predictions for the muon stopping power of PVT. Where T = Muon Kinetic Energy, p = Muon Momentum, Ionization, Brems, Pair prod, Photonucl = Stopping Power due to ionization, Bremsstrahlung, e^+e^- pair production and photonuclear interactions respectively, Total = Total Stopping Power, CSDA range = average muon path length travelled as it slows down to rest, according to the continuous-slowing-down approximation.

T	p [MeV/c]	Ionization	Brems	Pair prod	Photonucl	Total	CSDA range [g/cm^2]
				[MeV cm^2/g]			
10.0 MeV	4.704×10^1	7.917				7.917	7.062×10^{-1}
14.0 MeV	5.616×10^1	6.171				6.171	1.285×10^0
20.0 MeV	6.802×10^1	4.816				4.816	2.398×10^0
30.0 MeV	8.509×10^1	3.734				3.734	4.789×10^0
40.0 MeV	1.003×10^2	3.187				3.187	7.707×10^0
80.0 MeV	1.527×10^2	2.388				2.388	2.266×10^1
100. MeV	1.764×10^2	2.237				2.237	3.134×10^1
140. MeV	2.218×10^2	2.082				2.082	4.997×10^1
200. MeV	2.868×10^2	1.992				1.992	7.955×10^1
300. MeV	3.917×10^2	1.957			0.000	1.957	1.303×10^2
325. MeV	4.171×10^2	1.956			0.000	1.956	*Minimum ionization*
400. MeV	4.945×10^2	1.962			0.000	1.962	1.814×10^2
800. MeV	8.995×10^2	2.033	0.000		0.000	2.034	3.817×10^2
1.00 GeV	1.101×10^3	2.066	0.000		0.000	2.067	4.793×10^2
1.40 GeV	1.502×10^3	2.120	0.000		0.001	2.121	6.702×10^2
2.00 GeV	2.103×10^3	2.179	0.000	0.000	0.001	2.181	9.489×10^2
3.00 GeV	3.104×10^3	2.246	0.001	0.001	0.001	2.249	1.400×10^3
4.00 GeV	4.104×10^3	2.293	0.001	0.001	0.002	2.297	1.840×10^3
8.00 GeV	8.105×10^3	2.400	0.003	0.003	0.004	2.410	3.534×10^3
10.0 GeV	1.011×10^4	2.433	0.004	0.004	0.005	2.445	4.358×10^3
14.0 GeV	1.411×10^4	2.480	0.006	0.006	0.007	2.499	5.975×10^3
20.0 GeV	2.011×10^4	2.528	0.009	0.010	0.009	2.557	8.347×10^3
30.0 GeV	3.011×10^4	2.580	0.015	0.018	0.014	2.627	1.220×10^4
40.0 GeV	4.011×10^4	2.615	0.021	0.027	0.018	2.681	1.597×10^4
80.0 GeV	8.011×10^4	2.697	0.048	0.065	0.035	2.845	3.043×10^4
100. GeV	1.001×10^5	2.722	0.063	0.086	0.043	2.914	3.737×10^4
140. GeV	1.401×10^5	2.760	0.093	0.129	0.060	3.042	5.080×10^4
200. GeV	2.001×10^5	2.800	0.140	0.198	0.084	3.223	6.995×10^4
300. GeV	3.001×10^5	2.845	0.222	0.315	0.126	3.509	9.967×10^4
400. GeV	4.001×10^5	2.877	0.306	0.438	0.169	3.790	1.271×10^5
800. GeV	8.001×10^5	2.954	0.659	0.948	0.341	4.902	2.196×10^5
1.00 TeV	1.000×10^6	2.980	0.841	1.213	0.428	5.461	2.583×10^5
1.19 TeV	1.194×10^6	3.000	1.019	1.466	0.515	6.000	*Muon critical energy*
1.40 TeV	1.400×10^6	3.018	1.209	1.738	0.607	6.572	3.249×10^5
2.00 TeV	2.000×10^6	3.059	1.774	2.545	0.879	8.258	4.062×10^5
3.00 TeV	3.000×10^6	3.106	2.723	3.889	1.347	11.066	5.105×10^5
4.00 TeV	4.000×10^6	3.141	3.688	5.252	1.823	13.905	5.910×10^5
8.00 TeV	8.000×10^6	3.225	7.602	10.746	3.807	25.380	8.008×10^5
10.0 TeV	1.000×10^7	3.252	9.582	13.514	4.829	31.177	8.718×10^5
14.0 TeV	1.400×10^7	3.294	13.534	19.027	6.936	42.792	9.809×10^5
20.0 TeV	2.000×10^7	3.340	19.515	27.345	10.175	60.375	1.098×10^6
30.0 TeV	3.000×10^7	3.392	29.475	41.183	15.798	89.848	1.233×10^6
40.0 TeV	4.000×10^7	3.430	39.492	55.066	21.570	119.558	1.329×10^6
80.0 TeV	8.000×10^7	3.523	79.640	110.649	45.811	239.624	1.561×10^6
100. TeV	1.000×10^8	3.554	99.763	138.476	58.382	300.175	1.636×10^6

APPENDIX B: RAYSIM6.0

RaySim was produced by J.E. Cotter, "RaySim 6.0 - A Free Geometrical Ray Tracing Program for Silicon Solar Cells," Proceedings of the 31st PVSC, Lake Buena Vista, USA, January 3-7, 2005, in press." For full documentation, see http://www.pv.unsw.edu.au/Links/RaySim6/HomeOfRaySim6.htm.

RaySim is a free ray-tracing program for Windows based OSs. It was used to simulate scintillation light in a slab of scintillator and the absorption of this light by a PM or WLS bar. The results of which have been relied upon to decide which trigger design to recommend. There are many good qualities of RaySim that meant it has been suitable for this purpose

(a) It is free;
(b) It provides the user with significant control over the precision;
(c) It produces reproducible results;
(d) It records and totals the outcome of every ray in the simulation;
(e) It takes different light attenuation lengths and refractive indices of materials into account.

However, RaySim has several problems

(a) Point sources can only be produced in rectangular arrays in the x-y (z=0) plane;
(b) Rays from each point source have the same θ and φ distribution;
(c) Rays from each point source are not isotropically distributed over the surface of a sphere, rather RaySim produces a matrix of equally spaced θ and equally spaced φ (thus producing significantly more rays at the poles);
(d) Parameters can only be changed via the graphical interface;
(e) Only 13 'planes' per 'layer' can be made, 2 'planes' were required for a single surface and all sources must start in 'layer0'- see documentation.
(f) Simulations for many point sources are very time consuming.

The isotropy problem was the most significant for if it were not overcome then the RaySim program would have been useless. (a), (b) and (d) meant that one could not run simulations in a Monte-Carlo fashion summing over randomly positioned and angled (but isotropic over the surface of a sphere) rays. (e) meant that one could not even approximate curved surfaces.

The method used to get an isotropic ray distribution from RaySim was to run it with an array of point sources (70 in total for the scintillator, each in the centre of 50mm x 50mm square) that each emitted at one degree intervals in φ for a single value of θ. Simulations were then run with fixed parameters, each time adjusting θ (at 2.5 degree intervals) manually. The data for each θ value was exported to Excel and multiplied by the sinθ; this data was then summed to get the final result. This method was tested by creating a cube of perfect absorbers and looking for one sixth of rays to be absorbed by each face, the results of this are given in Table 9.

Table 9 Method Isotropy Test

Face	Percentage of Rays Absorbed	Discrepancy from Isotropy
Top/Bottom	16.8453%	0.1786%
North/South/East/West	16.5773%	-0.0894%

A maximum error of 0.18% in the isotropy of the results was deemed sufficiently small to run simulations at. Further checks were made after the simulations for the trigger were run to look for lost intensity due to rounding errors: from an expected intensity of 25200.000 rays, actual intensity for each θ (prior to multiplication by sinθ) was never out by more than ±0.001.

APPENDIX C: COMPANIES' CONTACT DETAILS

Scintillators

Eljen Technology, P.O. Box 870, 300 Crane Street, Sweetwater, Texas, USA, 79556, www.eljentechnology.com, churlbut@eljentechnology.com, Tel: 01 325 235 4276.

Saint-Gobain (Holland Office), P.O. Box 3093, 3760 DB Soest, The Netherlands, www.detectors.saint-gobain.com, frans.kniest@saint-gobain.com, Tel: 31 35 60 29 700.

Photomultipliers

Hamamatsu (UK Office), 2 Howard Court, 10 Tewin Road, Welwyn Garden City, Hertfordshire, AL7 1BW, www.hamamatsu.com, rsmith@hamamatsu.co.uk, Tel: 01707 294 888.

Sens-Tech, Bury Street, Ruislip, Middlesex, HA4 7TA, www.sens-tech.com, giselle.lord@sens-tech.com, Tel: 01895 630 771.

Photonis, Avenue Roger Roncier, B.P. 520, 19106 Brive Cedex, France, www.photonis.com, (UK Rep) j.harper@photonis.com, Tel: 01462 892 088.

Plastic Polishing

Engineering and Design Plastics, 84 High Street, Cherry Hinton, Cambridge, CB1 9HZ, www.edplastics.co.uk, sales@edplastics.co.uk, Tel: 01223 249 431.

NE Plastics, Unit 1 Ruxley Corner Industrial Estate, Edgington Way, Sidcup, Kent, DA14 5BL, www.neplastics.co.uk, sales@neplastics.co.uk, Tel: 02083 089 990.

REFERENCES

1. Birmingham Spark Chamber. [Online] [Cited: 2 September 2008.] http://www.ep.ph.bham.ac.uk/general/outreach/SparkChamber/.

2. *Cosmic Rays.* **C. Amsler, et al.** 2008, Physics Letters, Vol. B667.

3. *Muon Stopping Power and Range Tables 10 MeV-100 TeV.* **D.E. Groom, N.V. Mokhov, S.I. Striganov.** 2, July 2001, Atomic Data and Nuclear Data Tables, Vol. 78, pp. 183-356.

4. **Knoll.** *Radiation Detection and Measurement, Second Edition.* s.l. : John Wiley & Sons, Inc., 1989.

5. Eljen Technology Products. *Eljen Technology.* [Online] 2006. [Cited: 4 September 2008.] http://www.eljentechnology.com/products.html.

6. Saint-Gobain Plastic Scintillators. *Saint-Gobain.* [Online] 2008. [Cited: 4 September 2008.] http://www.detectors.saint-gobain.com/Data/Element/Node/Category/Category_edit.asp?ele_ch_id=C0000000000000001855.

7. Hamamatsu Photonics. [Online] [Cited: 10 September 2008.] http://sales.hamamatsu.com/en/home.php.

8. **Collaboration, ATLAS/Tile Calorimeter.** *Atlas Tile Calorimeter Technical Design Report.* s.l. : CERN, 1996.